The Pennsylvania State University

Schreyer Honors College

Department of Chemical Engineering

Modeling the Synergistic Effects of Combination Therapy for Glioblastoma Multiforme

Matthew Alexander Browe

Spring 2011

A thesis
submitted in partial fulfillment
of the requirements
of a baccalaureate degree
in Chemical Engineering
with honors in Chemical Engineering

Reviewed and approved* by the following:

Dr. Antonios Armaou
Associate Professor
Thesis Advisor

Dr. Wayne Curtis
Professor
Honors Advisor

Dr. Andrew Zydney
Department Head
Faculty Reader

*signatures are on file in the Schreyer Honors College office

Abstract

The Vital-Lopez model of a glioblastoma multiforme (GBM) tumor was modified to include haptotactic migration strategies and radiotherapeutic treatment methods. Haptotactic migration strategies in the model showed little improvement in overall tumor growth and this component likely will involve further modification with the parameters describing the dynamics of the coupled effects of extracellular matrix degradation and repair. Radiotherapy methods were analyzed against typical fractionation schemes with and without quiescent cell killing assumed and the model was tested against fractionation schemes *in vivo* as well. Assumption of quiescent cell killing provided the greatest fidelity with other models but did not accurately depict high-dose fractionation schemes. Lastly, analysis of the model against combination therapies *in vivo* confirmed a synergistic effect with concomitant temozolomide and radiotherapy and provides a template for future work investigating specific synergism parameters.

Table of Contents

Acknowledgements

I would like to acknowledge Dr. Francisco Vital-Lopez for helping me integrate my ideas with his existing project. His assistance in helping me to understand his previous work was tremendously valuable in helping me to advance the project, and his countless hours spent helping me solve any problems that arose in the course of my work are greatly appreciated. I would like to thank Dr. Antonios Armaou for his guidance as my thesis advisor and his tremendous patience with me as I undertook a challenging project.

I also wish to thank my parents, Andrew and Paula Browe, for being very supportive of me in anything I involved myself in as an undergraduate and for their guidance in helping me complete an unconventional route to a Chemical Engineering degree at Penn State. Lastly, I wish to thank my grandfather, Paul Laughner, for having always been a great fan, inspiration, and friend.

Chapter 1

Introduction

Glioblastoma multiforme (GBM) is among the most aggressive and challenging human cancers, accounting for 50-60% of primary brain tumors in adults (Mohin, 2006) and associated with a median survival of 10-12 months after diagnosis (Alford, 1991). Aside from its high resistance to conventional cancer treatments such as radiotherapy (Kleinsmith, 2006) and vulnerable region of genesis, the invasiveness of GBM tumor cells is primarily what has rendered it a very deadly disorder and why even seemingly complete surgical resection of the tumor fails uniformly. *In vivo* experimental results have verified this characteristic, as glioma cells have been identified throughout the central nervous system within 7 days of tumor xenograft implantation in a rat brain (Silbergeld, 1997).

The invasiveness of GBM tumor cells is largely due to three major mechanisms of migration: chemotaxis, haptotaxis, and cell-cell adhesion forces (Chen, 2009). Chemotaxis is cell migration up favorable chemical gradients in the extracellular space, haptotaxis is cell migration up gradients of soluble proteins in the extracellular space, and cell-cell adhesion forces mainly hinder movement of the cell and are most effective when neither strong local chemotactic gradients nor strong local haptotactic gradients exist (Chen, 2009). Chemotaxis is the primary determinant of cell migration, but haptotaxis plays a major role in migration strategies far from the tumor spheroid core (Chen, 2009). It is well-documented that in developmental processes involving haptotactic cell migration, a relatively small proportion of “trail-blazing” cells can act to guide others through their beaten path in the extracellular matrix (ECM) (Insall, 2006). The specific orientation of the ECM has been shown to be a significant determinant of the rate and heterogeneity of tumor invasion (Painter, 2009).

Glioblastoma is first treated through surgical resection of the tumor if feasible. Removal of 98% or more of the initial tumor cells with resection has been associated with notably longer life expectancy

than if fewer than 98% are removed (Lecroix, 2001). Nevertheless, recurrence of the tumor occurs uniformly due to GBM cells being present outside the removed area due to their invasive characteristics. Chemotherapeutic and radiotherapeutic treatments in patient-specific dosing schedules then become the primary therapeutic strategies.

Finding optimal treatments and treatment schedules for GBM is essential in progressing towards ultimately improving the survival rate and quality of life of patients who have been diagnosed with this devastating cancer. Mathematical modeling provides a necessary medium for developing models based on existing clinical data to rapidly test and predict the outcomes of future treatments. Many efforts have been made to accurately depict the rapidly invasive nature of the disease. In both *in vivo* and *in vitro* models, migrating tumor cells detach from the primary spheroid core early in tumor evolution and invade the surrounding brain (Guillamo, 2001). Simulation results have suggested that the ability of GBM cells to degrade the ECM and migrate through a permissive ECM are the primary factor in this tremendous degree of invasiveness (Eikenberry, 2009). Given these characteristics of invasion and treatment of GBM, this current study involves modifying cell migration algorithms by incorporating haptotactic effects to the Vital-Lopez glioblastoma tumor progression model (Vital-Lopez, 2010) and improving its applicability by including radiotherapeutic treatment.

Chapter 2

Simulation Methods

Haptotaxis

The first modification of the model involves incorporation of haptotactic gradients in the cell motility algorithm. The current Vital-Lopez model takes into account only chemotaxis as a source of cell migration, with oxygen as the only chemoattractant involved (Vital-Lopez, 2010). When strong local chemotactic gradients fail to exist, cell movement in the model assumes a biased random walk (Vital-

Lopez, 2010). While chemotaxis has been shown to be the predominant mechanism for determining migrating direction of GBM tumor cells, at low local chemotactic gradients, factors such as haptotaxis play a major role in cell motility (Chen, 2009).

The revised model takes into account haptotaxis forces in determining the overall local gradients for motility of each tumor cell. Haptotaxis involves the migration of tumor cells up gradients of soluble proteins in the extracellular matrix (ECM). This occurs biologically through cell surface heterodimers called integrins serving as ligands for tumor cells to bind to these regions of higher ECM protein concentration or adjacent cells (Bellail, 2004). Tumor cells at the invasive front detach from the primary tumor mass, adhere to the ECM via specific receptors, and locally degrade ECM components (Bellail, 2004). The migration capabilities of a tumor largely depend on the cell type, as each cell type has a different sensing radius that determines its ability to sense its local microenvironment (Kim, 2009).

Protein gradients exist naturally in the ECM *in* vivo, but these are created to a greater extent by invading tumor cells, as it has been well-documented that the ECM composition is changed by invading tumors (Rutka, 1988). These gradients are largely established by tumor cells through secretion of matrix metalloproteinases (MMPs) which and degrade the ECM (Kim, 2009). The synthesis of MMPs by the cells is thought to be a complex process regulated by several growth factors, cytokines, and hormones (Rooprai, 2000). MMP secretion rate of the cell plays a major factor in its migratory properties, as cells with higher MMP secretion rates have been shown to migrate faster from the tumor spheroid core (Kim, 2009). MMP activity has generally been found to be greater *in vitro* than *in vivo*, possibly due to MMPs being stimulated by local microenvironmental conditions *in vitro* but produced on demand in small quantities by enzymes *in vivo* (Rooprai).

Matrix degradation is either contact or non-contact dependent (Painter, 2009). In contact-dependent degradation, referred to as pericellular proteolysis, the MMPs are recruited to focal

adhesions at the leading edge of a migrating cell, acting on matrix fibres directly in the cell's path. In non-contact dependent degradation, MMPs are secreted into the immediate extracellular environment where they degrade the matrix.

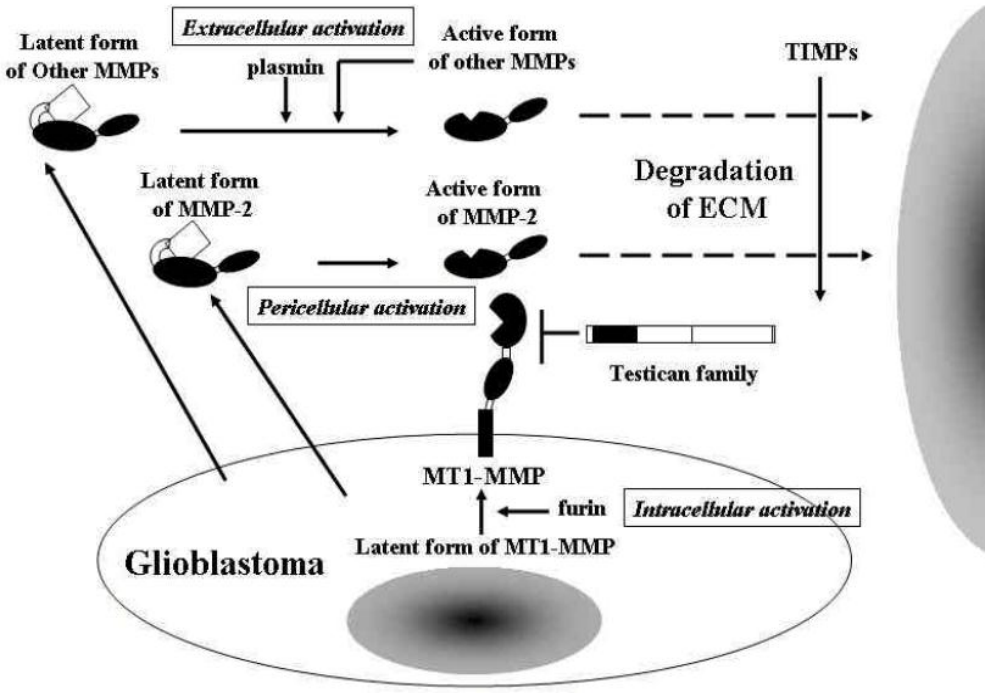

Figure I: MMP activation pathways (Nakada, 2003)

There are 8 distinct structural classes and 28 designations of MMPs (Egeblad, 2002), two of which have well-documented ECM degradation capabilities. MMP-2, also known as Gelatinase A, is activated on the cell surface in a pericellular manner in contact-dependent degradation. The other major degradory MMP, MMP-9, is secreted in the extracellular space in a latent precursor form, typical of most MMPs (Nakada, 2003). The activation pathways for each are shown in Figure I. Glioblastoma multiforme has consistently been associated with high expression of both MMPs (Gabelloni, 2010), but the revised Vital-Lopez model makes the simplying assumption that all matrix-degrading MMPs are secreted in the extracellular space in a non-contact dependent manner.

Haptotaxis, or haptotactic permission, is treated differently in different models. Some consider it as a non-diffusible tissue quality (Kim, 2009) with ECM-degrading MMPs as non-diffusible substances (Panovska, 2007), while others consider MMPs to be diffusing through the ECM throughout the degradation process (Kim, 2009). This study considers MMPs as diffusing substances, secreted solely by proliferating and migrating cells (Panovska, 2007) and with a spatiotemporal concentration distribution modeled by Equation 1, from Kim et al (Kim, 2009):

$$\frac{dP}{dt} = D_P \, \Delta P + \lambda_{31} n - \lambda_{32} P \qquad (1)$$

Where

P = MMP concentration in g/cm^3

D_P = MMP diffusion coefficient, 5.0*10^{-7} cm^2/s

λ_{31} = Production rate constant of MMPs by cells, 6.94*10^{-8}s^{-1}

n = Local tumor cell density in g/cm^3, calculated in the Vital-Lopez model

λ_{32} = Natural decay rate constant of MMPs, 5.0*10^{-6}s^{-1}

This study makes the simplifying assumption that cancer cells are the only source of MMPs and that initial concentrations of MMPs in the extracellular space are all zero, though this is not quite the case in reality (Egeblad, 2002). Having obtained the concentrations of MMPs using a function to solve the partial differential equation in (1), the model then determines the ECM spatiotemporal concentration from an ordinary differential equation, Equation 2, from Kim (Kim, 2009):

$$\frac{dp}{dt} = -\lambda_{21} P p + \lambda_{22} p(1 - \frac{p}{p_0}) \quad (2)$$

Where

ρ = Extracellular matrix density in g/cm^3

ρ_0 = Initial extracellular matrix density, 1*10^{-3} g/cm^3

λ_{21} = Degradation rate constant of the ECM in cm^3/g/s

λ_{22} = Reconstruction constant of the ECM, 5.0*10^{-6} s^{-1}

Initial conditions assume a homogenous ECM of density 1*10^{-3} g/cm^3, consistent with Kim's value. This assumption is valid for *in vitro* experiments but not *in vivo*, as a vastly heterogeneous environment is present in that setting. The model also assumes that invading cells do not completely degrade the ECM, as excessive degradation can inhibit rather than aid migration (Goldbrunner, 1999) (Mahesparan, 1999). Therefore, the ECM degradation rate constant from Kim is not used, as it rapidly caused complete degradation of the ECM in a short time period. Instead, this parameter was fit so that the limiting degree of degradation of the ECM at the initial MMP concentration, taken from Kim as 1*10^{-7} g/cm^3, was 50% of the original ECM density, ensuring only partial degradation would occur. Based on those guidelines, this value was determined to be λ_{21} = 25 cm^3/g/s, as opposed to the value of 3*10^8 cm^3/g/s used by Kim. The ECM concentration profile at a constant MMP concentration with this degradation constant is shown in Figure IX in the Appendix.

Radiotherapy

The next modification of the Vital-Lopez model involves incorporation of a radiation therapy scheme into the treatment schedule. The previous version of the model involved the chemotherapeutic

agent Temozolomide (TMZ) as the sole method of treatment (Vital-Lopez, 2010). The aim of radiation therapy in cancer treatment is to destroy cancer cells while limiting damage to nearby healthy cells (Oldham, 2001), and it is imperative that the fast proliferating tumor tissue is markedly more radiosensitive that the slow proliferation normal tissue for treatment to be effective (Cordes, 2004). Radiotherapy, while a common method to cure highly radiosensitive cancers such as lymphoma (Kleinsmith, 2006), is not as effective at treating glioblastoma (Kleinsmith, 2006). However, it has been shown to be more effective at delaying tumor growth than temozolomide alone in mice at biologically viable doses and demonstrated a variable synergy when given in combination therapy with TMZ (Kil).

Radiation therapy is typically administered in units of Gray, where 1 Gray is equal to 1 Joule of ionizing radiation absorbed per kilogram of patient body weight. Typically, radiation therapy is applied either to the whole brain or to the designated tumor volume with a 1-2 cm margin around the designated invasive edge (Eikenberry, 2009). Once radiation is absorbed by the cell, the fundamental mechanism for cell death, while not completely understood, involves linear energy transfer (Tilly, 1999) where highly energized particles emitted from the radioactive source ionize the atoms which make up the DNA of the tumor cells. This causes lesions that effectively damage the DNA and are manifested as double-stranded breaks. Radiation death occurs through either interphase death, where cells are directly killed through treatments in excess of 100 Gy, or the clinically relevant mitotic death, where cell death is contingent upon division and consists in loss of the capacity to divide (Gliemroth, 2003).

Patients typically receive radiation therapy in doses called fractions over a several week period, rarely exceeding 60 Gy total cumulative dose. The biologically relevant dose of radiation is around 1.0-2.5 Gy/day (Rockne, A mathematical model for brain tumor response to radiation therapy, 2009). Above the maximum tolerable dose, radiotherapy kills normal healthy cells at an unacceptable frequency and provides no net benefit for the patient. Low-frequency, high-dose schemes have been shown to be more

effective than high-frequency, low-dose schemes (Rockne, 2009), so the simulations were begun using schedules toward the higher end of the biologically relevant dose realm.

The fate of a single irradiated cell cannot be predicted with current mechanistic knowledge, and only survival probabilities can be assigned to a cell based on experimental data (Stamatakos, 2002). Thus, radiotherapy has been commonly modeled by equation (3), the linear quadratic equation, which expresses the surviving fraction of a population of cells after a given dosage of radiation (Enderling, 2010):

$$S = e^{-nd(\alpha+\beta d)} \tag{3}$$

where S is the surviving fraction from 0 to 1 of a given population of cells after n fractions of radiation of dosage d, in units of Gy/fraction. The parameters α and β are highly dependent on the type of tissue being treated and the phenotype of the cells comprising that tissue. These parameters are typically expressed for a tissue in terms of their relationship, termed the α/β ratio. For proliferating cancer cells in brain tissue, this ratio is commonly accepted as approximately equal to 10 (Rockne, 2009) (Garcia, 2006).

In the modified model, radiation death is assumed to be an instantaneous process, following current models (Rockne, 2010), as DNA damage from radiation usually leads to death of cells within the first 2-3 cell divisions after exposure (Thompson, 1969) (Perez, 1998). Other models explicitly make this assumption that cells die after exactly 2 mitotic divisions following exposure to radiation (Stamakos, 2006) (Antipas, 2004). Sub-lethal radiation damage is repairable by the cell within 60-70 min (Brenner, 1995), well within the 2.4 hour time step in the Vital-Lopez model, and thus this period of increased treatment sensitivity for the cell is considered a non-factor. Also, cells with equal access to oxygen are assumed to have equal probability of being killed, regardless of location relative to other cells, as assumed in other models (Rockne, 2009). Since the Vital-Lopez model is a continuous-discrete model

that treats cells as discrete entities rather than a continuous field, radiotherapy is simulated by assigning a random number between 0 and 1 to each cell. If the cell's assigned number is greater than the surviving fraction calculated in equation (3), the cell dies.

The model was first evaluated, without haptotactic modifications, for efficacy against generic fractionation schemes of radiotherapy used in other models (Dionysiou, 2006). The radiobiological parameters used in the radiation tests were $\alpha = 0.17$, $\beta = 0.02$, typical of a tumor with mutated p53 tumor repair protein (Haas-Kogan, 1996) (Stamakos, 2006) (Dionysiou, 2006), which is characteristic of 40-60% of GBMs (Wu). Also, the model was evaluated against results of *in vivo* radiation dosing schedules administered to athymic rats with intracranially implanted U87MG and U251MG xenografts (Ozawa, 2006) for a qualtitative analysis of its predictive effects.

Tumor cell phenotype plays a major role in response to radiotherapy, as migrating cells have been found to be more radioresistant than proliferating cells is some cell lines (Amberger). Also, efficacy of radiation against tumor cells is directly relation to the oxygen content of the cell, with radiation mostly ineffective against hypoxic cells (Steel, 1997) (Eikenberry, 2009). Thus, a parameter called the oxygen enhancement ratio (OER) is utilized (Antipas, 2004). Cells with a lower access to oxygen in the Vital-Lopez model, such as the quiescent cells, had their radiobiological parameters adjusted by a factor proportional to the OER, which is commonly taken to be about 2.7 (Antipas, 2004). The alpha parameter from equation (3) is divided by the OER, and the beta parameter is divided by the square of the OER, as employed in other models (Stamakos, 2006). Some models employ separate OER values for the α and β parameters, listing OER_α from 1.7 to 1.8 and OER_β from 3.0 to 3.5 (Chapman, 2003). The Vital-Lopez model utilized the OER of 2.7 for simulations of the fractionation schemes outlined previously to evaluate its effect on the relative efficacy of each scheme, with relevant radiobiological parameters for each cell line taken from Taghian (Taghian, 1992).

Synergistic effects

The final modification to the Vital-Lopez model consists of beginning analysis towards incorporation of an algorithm for the synergistic effect of combination therapy of temozolomide and radiotherapy on the GBM tumor. This allows for the model to be more applicable towards current GBM treatment strategies, as combination strategy is currently considered the standard method of treatment for patients not involved in a clinical trial (Mason, 2006). When considering the effect of combination therapy with chemotherapy and radiotherapy, two types of interaction may be expected to occur: independent cytotoxicity of each agent, and a radiosensitization effect of the chemotherapeutic agent (Chenoufi, 1998) (Barazzuol, 2010). Carlson has shown that if there is a sensitization effect of treatments with glioblastoma, a radiosensitization effect from the chemotherapeutic agent is the usual outcome and not vice-versa (Carlson, 2009). Other studies have confirmed this, suggesting that a significant synergistic effect does indeed occur when temozolomide is given with radiotherapy (Barazzuol, 2010).

Given that it has been shown only radiosensitization may occur and not chemosensitization in combination therapy for GBM, adjustment of the α and β parameters of the radiotherapy model is thus the only modification needed for modeling of synergistic effects. Thus, these parameters would be increased by a constant ratio to model the dynamics of the tumor. A previous study involving modeling the synergistic effect of TMZ and chemotherapy on a population of patients implemented a reduction of 75.2% in the α/β ratio (Barazzuol, 2010). The Vital-Lopez model handles the tumor on the individual cell level and thus would offer an intriguing medium to compare synergistic parameters.

There are several mechanisms through which TMZ could enhance radiosensitivity. TMZ may redistribute the cells into a radiosensitive phase of the cell cycle, as cells exhibit the greatest radiosensitivity in the M and G2 phases and the greatest radioresistance in the S phase (Stamatakos,

2002) (Antipas, 2004). TMZ may also increase the number of double-strand DNA breaks after radiation exposure. There are many mechanisms by which TMZ could simply weaken a cell and leave it more vulnerable to radiation-induced apoptosis, such as mutations in the DNA mismatch repair (MMR) pathway or immediate activation of methylguanine methyltransferase (MGMT) (Kaina, 2007). These situations could thus improve the efficacy of such a treatment.

The current Vital-Lopez model was evaluated against combination therapy schemes by first calculating tumor volumes assuming independent cytotoxicity of each agent. Results of studies by Kil (Kil) of U251 tumor xenograft implantation in nude mice and Carlson (Carlson, 2009) of intracranial implantation of GBM12 xenografts in mice were used. Radiobiological parameters for U251 were used to simulate treatment with the GBM12 cell line, with all other radiobiological parameters taken directly from Taghian.

Chapter 3

Results

Haptotaxis

Simulations were first performed to evaluate the effect of the strength of the haptotaxis gradient c in the modified Vital Lopez model for the overall migrating direction of the cell determined by equation 4:

$$d = g_o + bg_v + cg_h \quad (4)$$

Where d is the migrating direction, g_o is the oxygen gradient, g_v is the vascular endothelial growth factor gradient from Vital-Lopez, b is a constant equal to 0.625, and g_h is the new local haptotactic gradient.

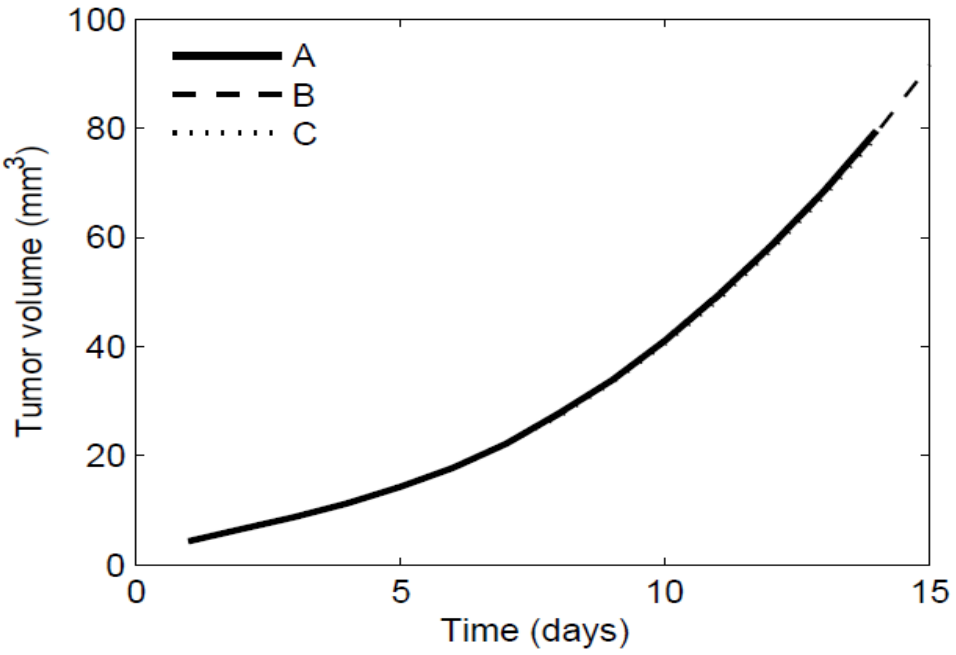

Figure II: Effect of haptotactic gradient strength on tumor volume. A: c = 0.1, B: c = 0.5, C: c = 1.0

Values of c of 0.1, 0.5, and 1.0 were chosen for the simulations. Tumor volume growth at each magnitude of the haptotaxis gradient is shown in Figure II. As shown, tumor growth had little effect on the strength of this gradient. Given the incredible invasive capacity of GBM, the haptotaxis parameter is likely to have a much stronger effect. Therefore, further analysis is required in terms of accurately describing the coupled dynamics of MMP secretion and ECM restoration in the tumor microenvironment so that stronger gradients are established. Sufficiently capturing this effect would allow for a sensitivity analysis of the haptotactic gradient strength parameter to tune it to experimental results and enable further analysis of haptotactic effects to proceed with the model.

Radiotherapy

Results of the typical fractionation schemes both without an oxygen enhancement ratio (OER) for quiescent cells and employing the OER for quiescent cells are shown in Figures III and IV, respectively. Exact fractionation schemes are defined in Table II in the Appendix. As expected,

incorporation of the OER into fractionation schemes yields lower tumor growth rates. The greatest effect is with the accelerated fractionation scheme, where tumor growth remains relatively stagnant for a few weeks, which is consistent with other models (Dionysiou, 2006). Both show that accelerated fractionation schemes of 2.0 Gy given twice a day achieves the highest cell killing rate and that hypofractionation achieves the worst tumor control. This is somewhat consistent with clinicial trials, as they have shown that accelerated fractionation improves tumor control rates for rapidly growing tumors (Perez, 1998), but hypofractionation schemes have been shown to achieve long duration of tumor control with less tumor cell kill. This is not reflected by the model, as the hypofractionation schemes of 6.0 Gy per day, administered once per week, yield the most rapidly growing tumors.

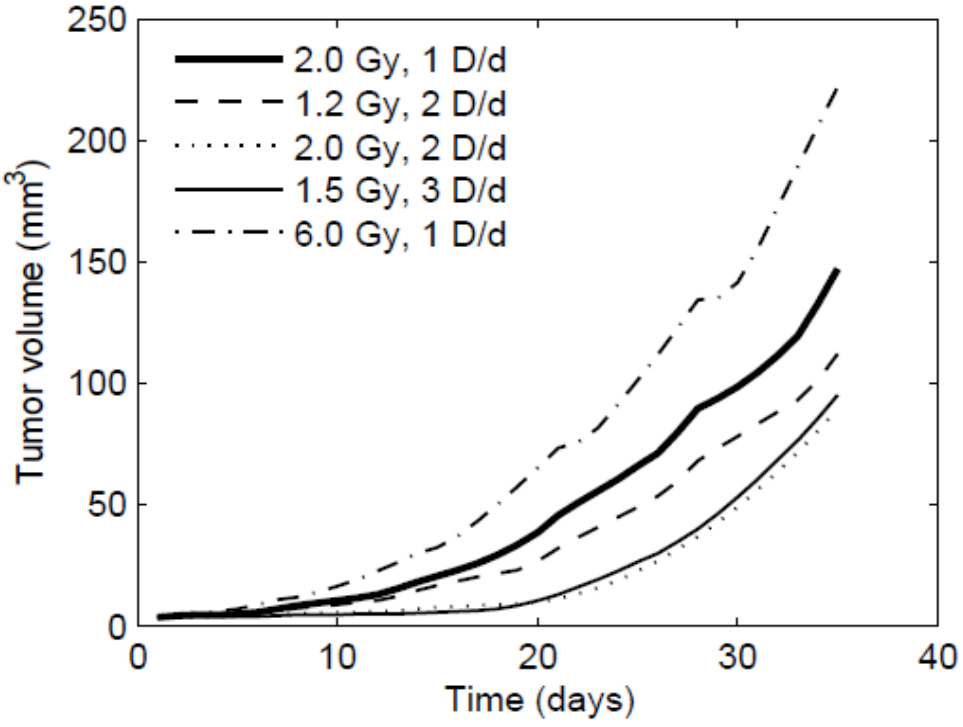

Figure III: Model simulations with different radiation fractionation schemes, not including an OER effect for killing of quiescent cells

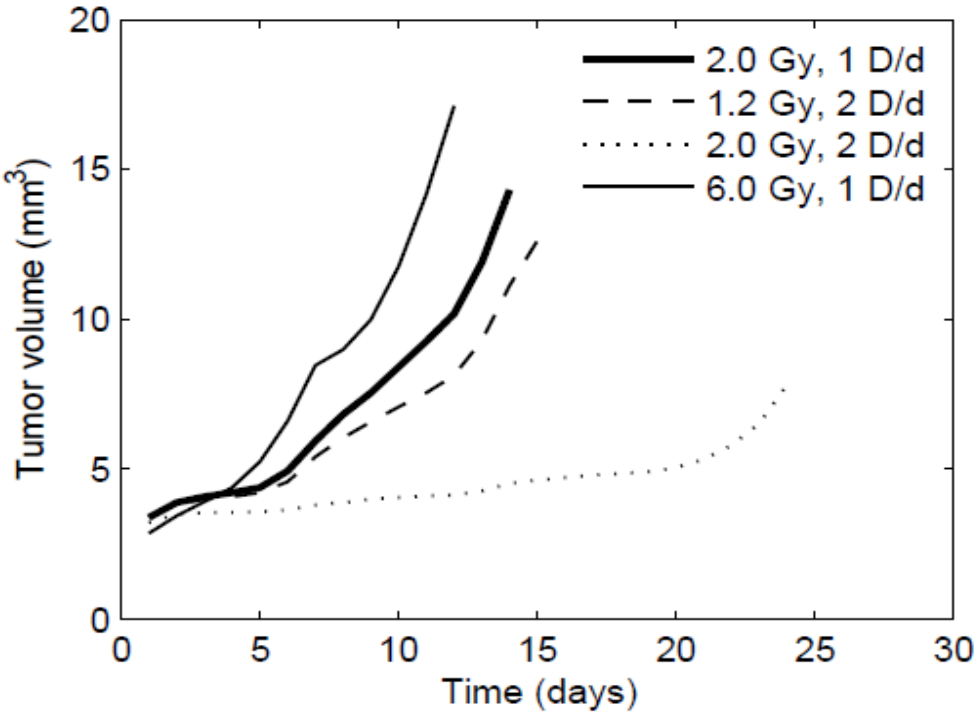

Figure IV: Model simulations with typical radiation fractionation schemes with an OER effect for killing of quiescent cells

The likely result of this is that developed radioresistance effects of the cell have not been taken into account. Complete analysis of the cell cycle could also be examined, as radioresistance has been largely determined to be cell cycle dependent (Antipas, 2004). Katzung (Katzung, 2001) has suggested that proliferating tumor cells spend their in various cell cycle phases in the following distribution: 40% in the G1 phase, 39% in the S phase, 19% in the G2 phase, and 2% in the M phase and, as mentioned previously, cells are most radioresistant in the S phase. It is possible that, just as TMZ could redistribute tumor cells into a radiosensitive phase, that certain fractionation schemes selectively redistribute tumor cells into a radioresistant phase. Both further analysis of potential developed resistance mechanisms in the GBM tumor cell and longer simulation trials are likely necessary.

The model was then tested against specific fractionation schemes in athymic rats invested by Ozawa. Simulation parameters are shown in Table I in the Appendix. Simulation models correctly predicted that for the U87mg cell line, 5 days of 3 Gy treatment yielded better tumor control than 10

days of 1Gy in terms of cumulative tumor volume, but not significantly. Treating 5 days of 2 Gy yielded slightly lower tumor growth than 10 days of 1 Gy, inconsistent with Ozawa's results, but simulations were not run for the duration of the experimental trials (35 days) and so further analysis is necessary. For the U251 cell line, the model correctly predicted that 10 days of 0.5 Gy treatment yields similar tumor growth as 5 days of 0.75 Gy treatment. It underestimate, however, the relative effects of the 5 day scheme of 1.5 Gy fractions, as this yielded the best tumor control in Ozawa's work but was outlasted by the 10 day treatment of 1 Gy/day in the modified Vital-Lopez model. Again, this suggests that acquired radioresistance/radiosensitization effects are involved and must be taken into account in the model.

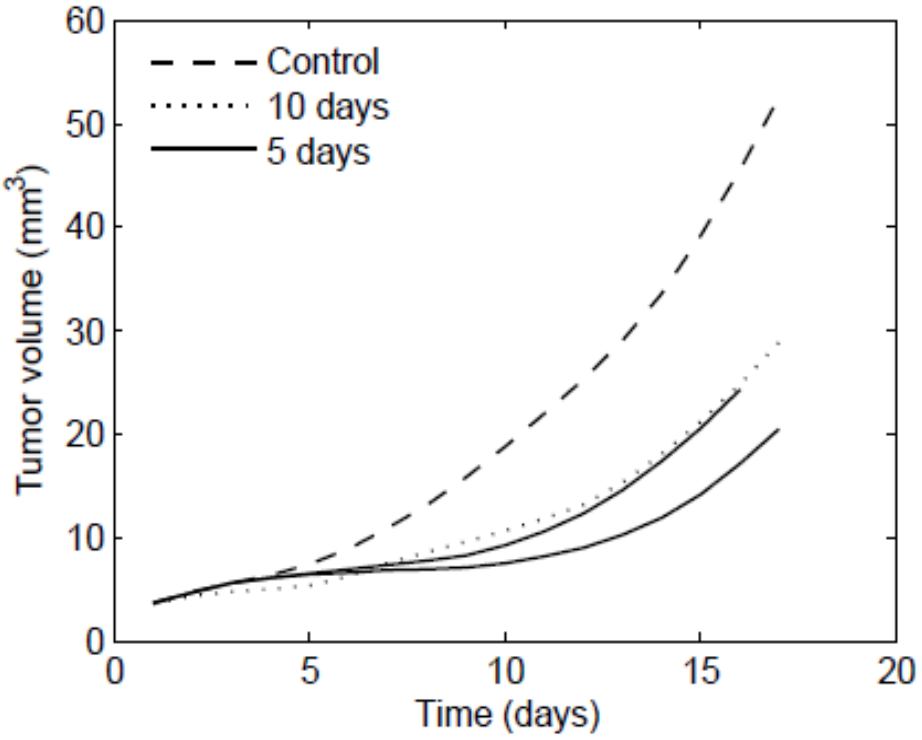

Figure V: Ozawa simulation results for U87mg trials

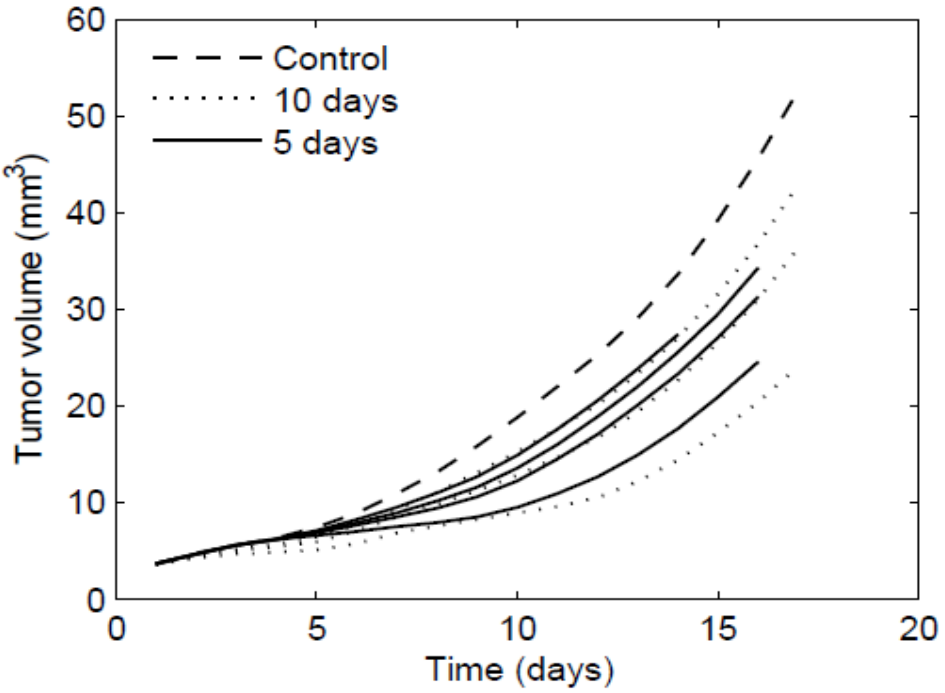

Figure VI: Ozawa simulation results for U251mg trials

Combination Therapy

Results from simulations from Carlson are shown in Figure VI. Simulation descriptions can be found in table I of the appendix. Simulation results show a similar efficacy of individual chemotherapy or radiotherapy, consist with experimental data, but suggest that sequential treatments of one week of temozolomide followed by one week of radiotherapy and one week of radiotherapy followed by one week of temozolomide impede tumor growth the longest. This was not the case, as concomitant temozolomide and radiotherapy was consistently found to have the greatest effect on hindering tumor progression experimentally. This suggests that independent cytotoxicity was not the prevailing mechanism of the two therapies and that synergistic effects were likely involved. It also shows a far more effective tumor control rate for sequential radiotherapy followed by chemotherapy. Simulations

would likely need to be run for a longer period of time to evaluate whether this treatment ultimately yielded different tumor characteristics or not.

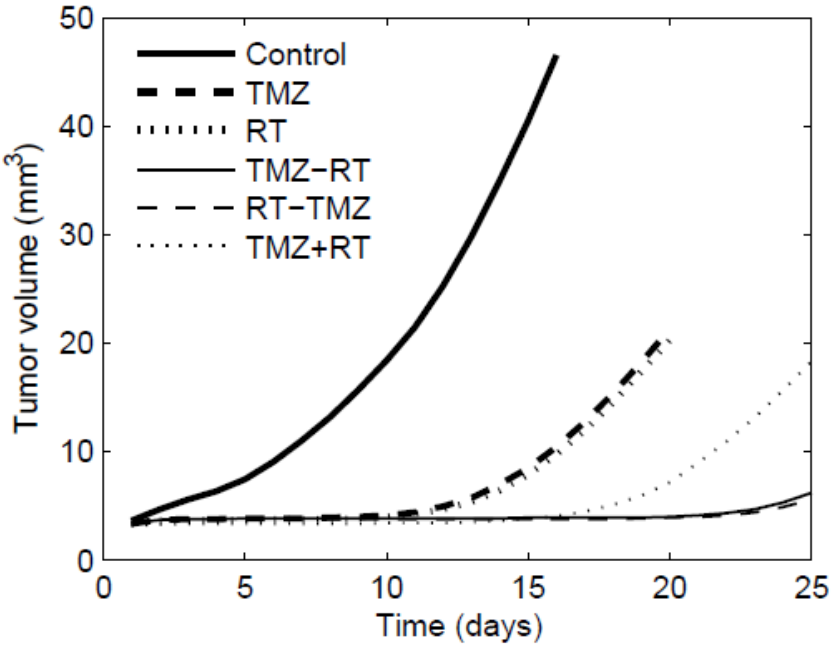

<u>Figure VII</u>: Results of Carlson simulations. TMZ = temozolmide applied, RT = radiotherapy applied, TMZ-RT = temozolomide then radiotherapy, RT-TMZ = radiotherapy then temozolomide, TMZ + RT = concomitant temozolomide and radiotherapy

Results from the Kil simulations are shown in Figure VII. Temozolomide treatment and radiation treatment individually are both shown to have a marginal effect on tumor growth, which is consistent with the nude mice data, though radiation treatment was slightly more effective in that setting. The combination therapy scheme in the simulation, however, only has a slightly greater effect on the relative reduction in tumor volume. Nude mice in Kil's work, shown in Figure VIII, experienced a significant reduction in relative tumor volume of over 90% of that of the untreated tumor at day 15, while the modified Vital-Lopez simulation predicts just a 35% reduction with its assumption of independent cytotoxicity. Thus, significant synergistic effects have been shown to occur with this treatment.

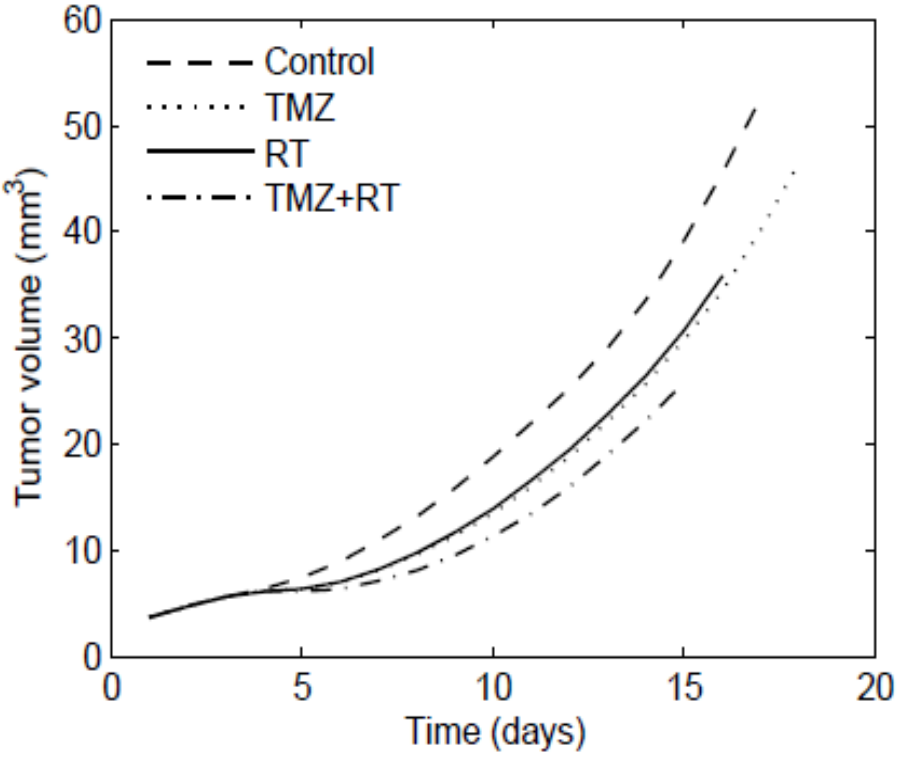

<u>Figure VIII</u>: Simulations results using the Kil experimental data. TMZ = 1 dose of 10 mg/kg TMZ in mice, RT = 1 fraction of 5 Gy, TMZ + RT = 1 dose of 10 mg/kg TMZ followed 1 hour later by 1 fraction of 5 Gy

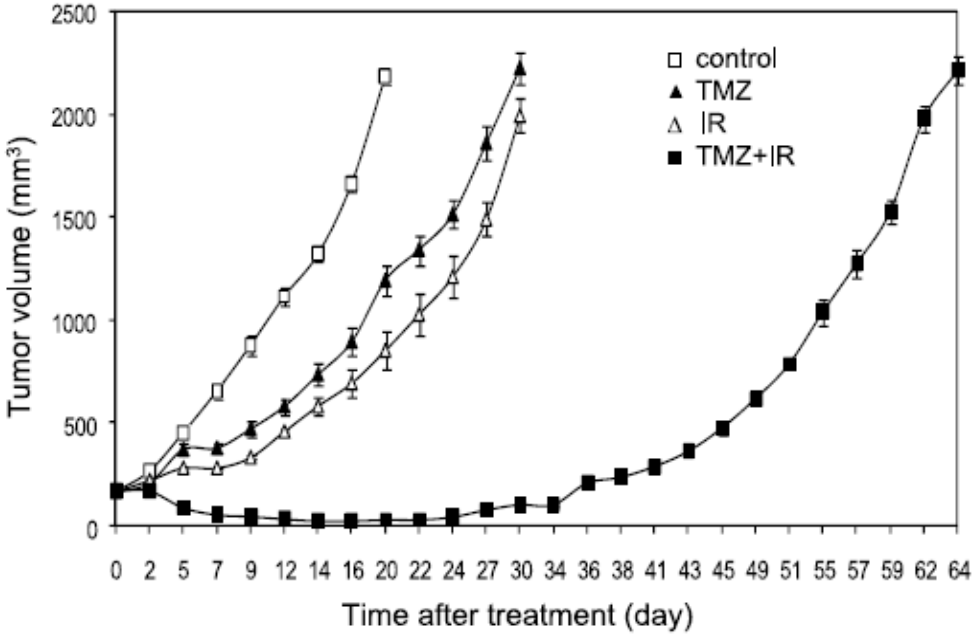

<u>Figure IX</u>: Kil experimental results using same dosing schedules

Chapter 5

Future Work

The incorporation of haptotactic permission and radiotherapeutic treatment adds fidelity to the current Vital-Lopez model and makes it more relevant in analyzing current treatment strategies employed for GBM. Nevertheless, aside from the modifications suggested from the simulation results, there are several directions that could be taken to further improve the model on both accounts. The current model assumes that radiotherapy has no effect on the extracellular matrix of the brain. This may not be the case, as radiation has been shown to cause fibrosis effects in organs such as the lung (Bentzen, 1996). If radiation-induced fibrosis occurred to a measurable extent in the extracellular space in the brain under certain conditions, haptotactic effects would be enhanced and cell migration would increase. Radiation therapy has been found to enhance cell motility in some cases (Zhai, 2006), and this hypothesis could be used to further investigate those circumstances.

Another potential direction for the project to proceed in involves incorporation of inhibitory agents in the treatment simulations. Methylguanine methyltransferase (MGMT) inhibitors such as O6-benzylguanine have been used frequently in treatment with TMZ and radiation with mixed effects on the sensitivity of each treatment (Wedge, 1997). Accurately modeling the relationship between these three agents in combination would improve the relevance of the Vital-Lopez model to current treatment strategies. The incorporation of radiotherapy also allows for the possibility of modeling advanced radiotherapeutic treatment strategies such as brachytherapy. In brachytherapy, radioactive “pellets” are implanted into the brain tumor, allowing for higher local radiation dosages to be distributed (Loeffler, 1990). Modeling the spatial distribution and apoptotic effect of radiation dosage in brachytherapy would increase the applicability of the model to different treatments.

Lastly, the haptotactic migration component of the model could be modified. The current model assumes secretion of MMPs with degradation by normal cells, but in reality, this degradation occurs from expression of tissue inhibitors of MMPs (TIMPs) by the normal brain cells (Placeholder1). Ultimately, the balance between MMPs and TIMPs is critical for control of glioma cell invasion (Planchenault, 2001). Also, not all MMPs promote tumor progression, as certain MMPs actually inhibit tumor growth and malignant transformation and cause antiangiogenic effects (Gabelloni, 2010). The efficacy of TIMPs is in question as well, though, as some studies have shown that decreased TIMP levels seen in glioblastoma could be insufficient to prevent most ECM destruction and cell invasion (Mohanam, 1995). The model could be improved to accurately predict the conditions under which TIMPs are secreted by the healthy brain cells, more accurately establishing haptotactic gradients and adding fidelity to the model.

Chapter 6

Conclusions

The Vital-Lopez model for tumor progression has been modified successfully with radiotherapeutic treatment schemes and has been given a foundation for a successful incorporation of haptotactic effects with some tuning of parameters. Radiotherapeutic treatment effects largely agree with literature data except for sequential treatment prior to temozolomide and high-dosage fractionation, both of which should be investigated in the future. It successfully predicts significant synergism against literature data and allows for future work in tuning radiobiological parameters to accurately capture these effects. Despite advances in prediction of glioblastoma treatment through the Vital-Lopez model and others, though, GBM remains a deadly disease with a poor prognosis. However, continuous developments in treatment schemes yield hope that it may be more manageable in the future. Mathematical modeling will undoubtedly serve as a useful tool for developing these treatments and optimizing them on an individual basis in the hope of maximum survival period and quality of life.

Appendix

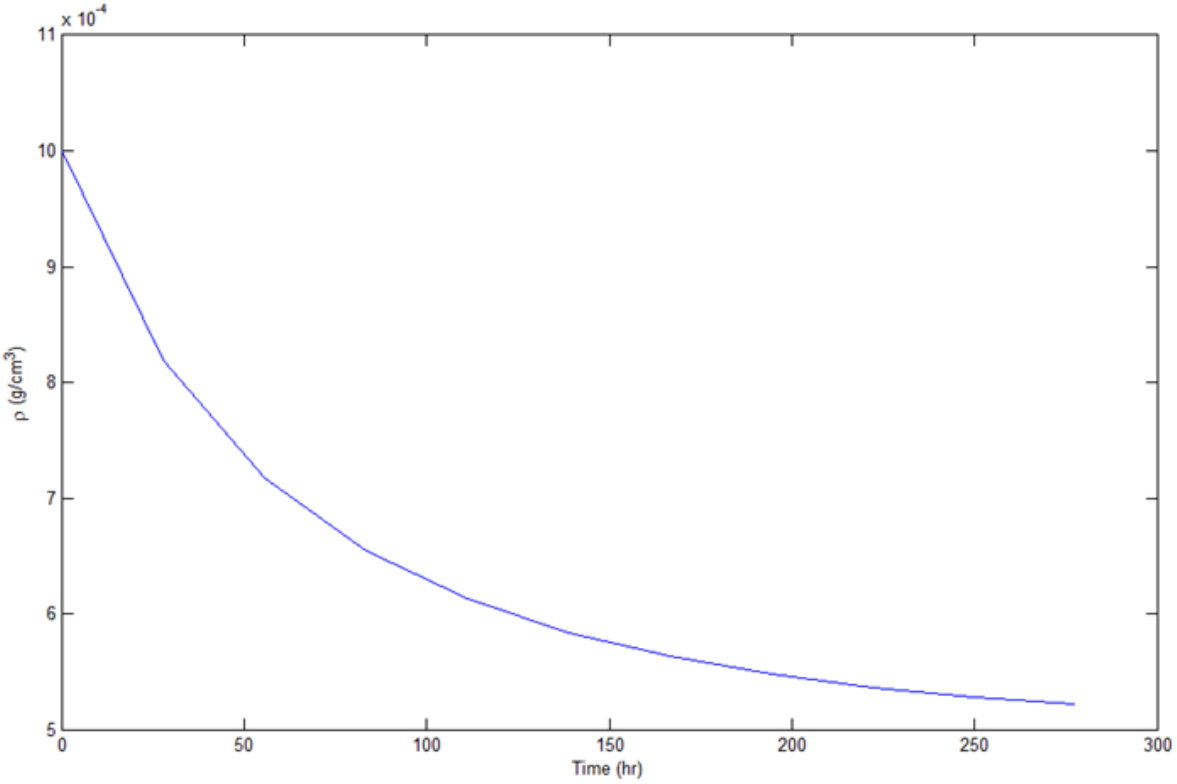

<u>Figure X</u>: Temporal ECM density profile at initial secreted MMP concentration from Kim

Table I: RT and Combination Therapy Dosing Simulations

Tumor	Days TMZ	TMZ (mg/kg)	Days RT	RT (Gy)	RT dose/day
Ozawa: Intracranial tumors in athymic rats					
U251	-	0	-	0	-
U251	-	0	1 to 5 and 8 to 12	0.3	1
U251	-	0	1 to 5 and 8 to 12	0.5	1
U251	-	0	1 to 5 and 8 to 12	1	1
U87[a]	-	0	-	0	-
U87	-	0	1 to 5 and 8 to 12	1	1
U251[a]	-	0	-	0	-
U251	-	0	1 to 5	0.5	1
U251	-	0	1 to 5	0.75	1
U251	-	0	1 to 5	1	1
U251	-	0	1 to 5	1.5	1
U87[a]	-	0	1 to 5	0	-
U87	-	0	1 to 5	2	1
U87	-	0	1 to 5	3	1
Kil: tumor implanted in legs of female nude mice					
U251[a]	-	0	-	0	-
U251	1	10	1	0	1
U251	1	0	1	4	1
U251	1	10	1	4	1
Carlson: intracranial tumor; mice					
GBM12[a]*	-	0	-	0	-
GBM12	1 to 5	66	-	0	-
GBM12	-	0	1 to 5	2	2
GBM12	8 to 12	66	1 to 5	2	2
GBM12	1 to 5	66	8 to 12	2	2
GBM12	1 to 5	66	1 to 5	2	2

a = rerun of first simulation, one set of results used to represent untreated tumor

*U251 cell line radiobiological parameters from Taghian were used

Table II: Radiotherapy fractionation simulations

Type of fractionation	OER	Days RT	RT (Gy)	RT dose/day
Standard fractionation	No consideration	1:5,8:12,15:19,22:26,29:33,36:40	2	1
Hyperfractionation	"	1:5,8:12,15:19,22:26,29:33,36:40	1.2	2
Acceleration fractionation	"	1:5,8:12,15:19	2	2
Accelerated hyperfractionation	"	1:5,8:12,15,16	1.5	3
Hypofractionation	"	1,8,15,22,29,36,43,50,57,64	6	1
Standard fractionation	2.7	1:5,8:12,15:19,22:26,29:33,36:40	2	1
Hyperfractionation	2.7	1:5,8:12,15:19,22:26,29:33,36:40	1.2	2
Acceleration fractionation	2.7	1:5,8:12,15:19	2	2
Accelerated hyperfractionation	2.7	1:5,8:12,15,16	1.5	3
Hypofractionation	2.7	1,8,15,22,29,36,43,50,57,64	6	1

References

Alford, E. C., et al. (1991). *The Pathology of the Aging Human Nervous System.* Philadelphia: Lea and Febiger.

Amberger, V., et al. Spreading and migration of human glioma and rat C6 cells on central nervous system myelin in vitro is correlated with tumor malignancy and involves a metalloproteolytic activity. *Cancer Research , 58*, 149-158.

Antipas, V., et al. (2004). A spatio-temporal simulation model of the response of solid tumours to radiotherapy in vivo: parametric validation concerning oxygen enhancement ratio and cell cycle duration. *Physics in Medicine and Biology , 49*, 1485-1504.

Barazzuol, L., et al. (2010). A mathematical model of brain tumour response to radiotherapy and chemotherapy considering radiobiological spects. *Journal of Theoretical Biology , 262*, 553-565.

Bearer, E. L., et al.(2009). Multiparameter Computational Modeling of Tumor Invasion. *Cancer Research , 69*, 4493-4501.

Bellail, A., et al. (2004). Microregional extracellular matrix heterogeneity in brain modulates glioma cell invasion. *International Journal of Biochemistry and Cell Biology , 36*, 1046-1069.

Bentzen, S. M., et al. (1996). Radiotherapy-Related Lung Fibrosis Enhanced by Tamoxifen. *Journal of the National Cancer Institute , 88*, 918-922.

Brenner, D., et al. (1995). A convenient extension of the linear quadratic model to include redistribution and reoxygenation. *International Journal of Radiation Oncology, Biology, and Physics , 32*, 379-390.

Carlson., et al. (2009). Radiosensitizing effects of TMZ observed in vivo only in a subset of MGMT methylated GBM xenografts. *Int J Radiat Oncol Biol Phys. , 75*, 212-219.

Chapman, J., et al. (2003). Single-hit mechanism of tumor cell killing by radiation. *International Journal of Radiation Biology , 79*, 71-81.

Chen, L. L., et al. (2009, March). Cancer Cell Motility: Optimizing Spatial Search Strategies. *Biosystems* .

Chenoufi., et al. (1998). In Vivo Demonstration of Synergy Between Radionuclide and Chemotherapy. *Journal of Nuclear Medicine , 39*.

Cordes, N., et al. (2004). Integrin signaling and the cellular response to ionizing radiation. *Journal of Molecular Histology , 35*, 327-337.

Dionysiou, D., et al. (2006). A computer simulation of an in vivo tumour growth and response to radiotherapy: New algorithms and parametric results. *Computers in Biology and Medicine , 36*, 448-464.

Egeblad, M., et al. (2002). New Functions for the Matrix Metalloproteinases in Cancer Progression. *Nature Reviews , 2*, 161-174.

Eikenberry, S., et al. (2009). Virtual glioblastoma: growth, migration, and treatment in a three-dimensional mathematical model. *Cell Proliferation , 42*, 511-528.

Enderling, et al. (2010). Quantitative Modeling of Tumor Dynamics and Radiotherapy. *Acta Biotheoretica , 58*, 341-353.

Gabelloni, P., et al. (2010). Inhibition of Metalloproteinases Derived from Tumours: New Insights in the Treatment of Human Glioblastoma. *Neuroscience , 168*, 514-522.

Garcia, L., et al. (2006). Fitting the linear-quadratic model to detailed data sets for different dose ranges. *Physics in Medicine and Biology , 51*, 2813-2823.

Gliemroth, J., et al. (2003). Proliferation, migration, and invasion of human glioma cells exposed to fractionated radiotherapy in vitro. *Neurosurgery Reviews , 26*, 198-205.

Goldbrunner, R., et al. (1999). Cell-extracellular matrix interaction in glioma invasion. *Acta Neurochirurgica , 141*, 295-305.

Guillamo, J., et al. (2001). Migration pathways of human glioblastoma cells xenografted into the immunosuppressed rat brain. *Journal of Neurooncology , 52*, 205-215.

Guo, A. C., et al. (2002). Lymphomas and high-grade astrocytomas: comparison of water diffusibility and histologic characteristics. *Radiology , 224*, 177-183.

Haas-Kogan, D., et al. (1996). p53-dependent G1 arrest and p53 independent apoptosis influence the radiobiologic response of glioblastoma. *International Journal of Radiation Oncology Biology Physics , 36*, 95-103.

Insall, R., et al. (2006). Moving matters: signals and mechanisms in directed cell migration. *Nat Cell Biol , 8*, 776-779.

Kaina, B., et al. (2007). MGMT: Key node in the battle against genotoxicyt, carcinogenicity and apoptosis induced by alkylation agents. *DNA Repair , 6*, 1079-1099.

Katzung, B., et al. (2001). *Basic and Clinical Pharmacology* (8th ed.). New York: McGraw-Hill.

Kil, W. J., et al. In Vitro and In Vivo Radiosensitization Induced by the DNA methylating Agent Temozolomide.

Kim, et al. (2009). A mathematical model for pattern formation of glioma cells outside the tumor spheroid core. *Journal of Theoretical Biology , 260*, 359-371.

Kleinsmith, L. J., et al. (2006). Principles of Cancer Biology. San Francisco: Pearson Education.

Lecroix, M., et al. (2001). A multivariate analysis of 416 patients with glioblastoma multiforme: prognosis, extent of resection, and survival. *Journal of Neurosurgery , 95*, 190-198.

Loeffler, J., et al. (1990). Results of Stereotactic Brachytherapy used in the Initial Management of Patients with Glioblastoma. *Journal of the National Cancer Institute , 82*, 1918-1921.

Mahesparan, R., et al. (1999). Extracellular matrix-induced cell migration from glioblastoma biopsy specimens in vitro. *Acta Neuropathologica , 97*, 231-239.

Mason, W., et al. (2006). Radiotherapy with Concurrent and Adjuvant Temozolomide: A New Standard of Care for Glioblastoma Multiforme. *Progress in Neurotherapeutics and Neuropsychopharmacology , 1*, 37-52.

Mohanam, S., et al. (1995). Expression of tissue inhibitors of metalloproteinases: negative regulator of human glioblastoma in vivo. *Clinical Experimental Metastasis , 13*, 57-62.

Mohin, G., et al. (2006). Glioblastoma Multiforme: advances in postsurgical management. *Community Oncology , 3*, 678-684.

Nakada, M., et al. (2003). The Role of Matrix Metalloproteinases in Glioma Invasion. *Frontiers in Bioscience* , 261-269.

Oldham, M., et al. (2001). Radiation physics and application in therapeutic medicine. *Journal of Physics Education , 36*, 460-467.

Ozawa, T., et al. (2006). Response of Intracerebral Human Glioblastoma Xenografts to Multifraction Radiation Exposures. *International Journal of Radiation Oncology, Biology, and Physics , 66*, 263-270.

Painter, K., et al. (2009). Modelling cell migration strategies in the extracellular matrix. *Journal of Mathematical Biology , 58*, 511-543.

Panovska, J., et al. (2007). Mathematical Model for Glioma Cell Invasion.

Perez, C., et al. (1998). *Principles and Practice of Radiation Oncology.* Philadelphia: Lippincott-Raven.

Planchenault, T., et al. (2001). Differential expression of laminin and fibronectin and of their related metalloproteinases in human glioma cell lines: relation to invasion. *Neuroscience Letters , 299*, 140-144.

Rockne, R., et al. (2009). A mathematical model for brain tumor response to radiation therapy. *Journal of Mathematical Biology , 58*, 561-578.

Rockne, R., et al. (2010). Predicting the eficacy of radiotherapy in individual glioblastoma patients in vivo: a mathematical modeling approach. *Physics in Medicine and Biology , 55*, 3271-3285.

Rooprai, H., et al. Proteases and their inhibitors in human brain tumours: a review. *Antitcancer Research , 13*, 1153-1157.

Rooprai, H., et al. (2000). The effect of exogenous growth factors on matrix metalloproteinase secretion by human brain tumour cells. *British Journal of Cancer , 82*, 52-55.

Rutka, J., et al. (1988). The extracellular matrix of the central and peripheral nervous systems: structure and function. *Journal of Neurosurgery , 69*, 155-170.

Saksena, S., et al. (2010). Predicting SUrvival in Glioblastomas Using Diffusion Tensor Imaging Metrics. *Journal of Magnetic Resonance Imaging , 32*, 788-795.

Silbergeld, D., et al. (1997). Isolation and characterization of human malignant glioma cells from histologically normal brain. *Journal of Neurosurgery , 86*, 525-531.

Stamakos, G., et al. (2006). A four-dimensional computer simulation model of the in vivo response to radiotherapy of glioblastoma multiforme: studies on the effect of clonogenic cell density. *The British Journal of Radiology , 79*, 389-400.

Stamatakos, G. S., et al. (2002). In Silico Radiation Oncology: Combining Novel Simulation Algorithms with Current Visualization Techniques. *Proceedings of the IEEE , 90*, 1764-1777.

Steel, G., et al. (1997). *Basic Clinical Radiobiology.* London: Arnold.

Taghian, A., et al. (1992). In vitro intrinsic radiation sensitivity of glioblastoma multiforme. *International Journal of Radiation Oncology, Biology, and Physics , 23*, 55-62.

Thompson, L., et al. (1969). Proliferation kinetics of X-irradiated mouse L cells studied with time-lapse photography. *Int J Radiat Biol , 15*, 347-362.

Tien, R., et al. (1994). MR imaging of high-grade cerebral gliomas: value of diffusion-weighted echoplanar pulse sequences. *American Journal of Roentgenology , 162*, 671-677.

Tilly, N., et al. (1999). Comparison of cell survival models for mixed LET radiation. *Internation Journal of Radiation Biology , 75*, 233-243.

Vital-Lopez, F., et al. (2010). Modeling the effect of chemotaxis on glioblastoma tumor progression. *American Institute of Chemical Engineers Journal , 57*, 778-792.

Wedge, S., et al. (1997). In vitro evaluation of temozolomide combined with X-irradiation. *Anticancer Drugs , 8*, 92-97.

Wu, J., et al. Frequency of p53 tumor suppressor gene mutations in human primary brain tumors. *Neurosurgery , 33*, 824-830.

Yamasaki, F., et al. (2010). Gliioblastoma treated with postoperative radio-chemotherapy: Prognostic value of apparent diffusion coefficient at MR imaging. *European Journal of Radiology , 73*, 532-537.

Zhai, G. G., et al. (2006). Radiation enhances the invasive potential of primary glioblastoma cells via activation of the rho signaling pathway. *Journal of Neuro-Oncology , 76*, 227-237.

Ziu, M., et al. (2006). Glioma-produced extracellular matrix influences brain tumor tropism of human neural stem cells. *Journal of Neuro-Oncology , 79*, 125-133.

Academic Vita of Matthew A. Browe

mab5735@psu.edu

Campus Address
925 Bellaire Avenue Apt Y220
State College, PA 16801

Permanent Address
65 Shady Drive
Indiana, PA 15701

Education

Bachelor of Science, Chemical Engineering

The Pennsylvania State University, University Park, PA, May 2011

Honors in Chemical Engineering

Honors Thesis Title:

Modeling the Synergistic Effects of Combination Therapy for Glioblastoma Multiforme

Thesis Supervisor: Dr. Antonios Armaou

Work Experience

Chemical Engineer (Intern) May 2010 to August 2010

Edgewood Chemical and Biological Center

Aberdeen Proving Ground, MD

Computer and Language Skills

MATLAB

Mathematica

C++ programming language

Spanish (verbal and written competency)

HYSYS process modeling software

Microsoft Office (proficient in Word, Excel, Powerpoint, and Visio)

ProPlan virtual refinery development software

Awards

Science, Mathematics, and Research for Transformation (SMART) Scholarship – June 2009

U.S. Department of Defense